The Effect of Boreal Late Autumn Snow Cover over Western and Central China on the Northern Hemisphere Wintertime Blocking Frequency

YEON-WOO CHOI AND JOONG-BAE AHN

Division of Earth Environmental System, Pusan National University, Busan, South Korea

ABSTRACT

The impact of snow cover in western and central China during late autumn on wintertime blocking occurrence is investigated using reanalysis data. The study results show that wintertime atmospheric circulations affected by late autumn snow cover anomalies form favorable conditions for increased blocking frequency (BF), especially in the North Pacific and North Atlantic. Evidence is also presented that the stratosphere–troposphere interactions are the key mechanism of the lag response of wintertime North Pacific and North Atlantic BFs to the late autumn snow cover. That is, positive anomalous snow cover can induce a dipole anomaly in the geopotential height field over the lower stratosphere, due to the decrease of the 300–1000-hPa thickness and the concurrent variation between the East Asian plateau jet and the polar front jet. The associated positive geopotential height anomalies are located over northwestern Eurasia. Meanwhile, western and central China shows remarkably negative geopotential height anomalies. Also, the corresponding atmospheric circulation in the lower stratosphere increases the Eliassen–Palm flux that propagates into the stratosphere through the constructive interference between the forced and climatological waves. The upward wave activity fluxes collapse the polar vortex in the stratosphere, resulting in the downward propagation of the geopotential and wind anomalies from the stratosphere. Consequently, the decreased zonal wind speed in the upper layer of the blocking region forms conditions favorable for wintertime blocking.

1. Introduction

Blocking is a large-scale atmospheric phenomenon that frequently occurs in the midlatitude westerly wind belt and is associated with the development of anticyclones in high latitudes, leading to stagnant movements of atmospheric pressure fields (Lejenäs and Økland 1983; Tibaldi and Molteni 1990; Barriopedro et al. 2006; You and Ahn 2012). The blocking phenomenon mainly occurs over the northeastern boundaries of the Pacific and Atlantic Oceans (Rex 1950b; Lejenäs and Økland 1983; Dole and Gordon 1983; Park and Ahn 2014). In particular, blocking exhibits high intensity and occurs widely during winter due to the large temperature difference between land and ocean (Rex 1950a,b; Charney et al. 1981; Colucci and Alberta 1996; He et al. 2014). According to previous studies, Northern Hemisphere blocks are linked to the anomalous structures of atmospheric variables such as temperature, geopotential height, and zonal wind component. These blocks show a highly concurrent relationship with local weather and climate (You and Ahn 2012; Park and Ahn 2014). In particular, blocking appearing in the Northern Hemisphere is related to extreme events such as cold spells, heat waves, heavy precipitation, and droughts (e.g., Hoskins and Sardeshmukh 1987; Black et al. 2004; Trigo et al. 2005; Buehler et al. 2011).

However, the mechanisms of the formation and maintenance of blocking are controversial because a variety of factors are known to act on blocking, such as nonlinear effects of atmospheric motion, orographic effects, tropical forcing, and energy supply by baroclinic transient eddies (Shutts 1983; Mullen 1987; Nakamura and Wallace 1993). Kung et al. (1990) insisted that global sea surface temperature anomalies are related to blocking frequency (BF) based on model experiments. Renwick and Wallace (1996) have shown that the phases of El Niño–Southern Oscillation are highly related with North Pacific BF on the interannual time scale, and Renwick (1998) has argued that southeast Pacific BF

Corresponding author: Joong-Bae Ahn, jbahn@pusan.ac.kr

increases in El Niño years but decreases in La Niña years. These studies have indicated that the evolution mechanism of blocking can also be related to the propagation of Rossby waves generated by anomalous tropical heating (Hoskins and Ambrizzi 1993; Tyrrell et al. 1996; Ambrizzi and Hoskins 1997; Kim and Ahn 2015). Also, several studies (Shabbar et al. 2001; Luo 2005; Barriopedro et al. 2006) have indicated that the phases of the North Atlantic Oscillation (NAO), the regional manifestation of Arctic Oscillation (AO; e.g., Sun and Ahn 2015), are closely related to the formation and maintenance of North Atlantic blocking. Song and Robinson (2004) and Woollings et al. (2010) have also indicated that stratospheric sudden warming (SSW) could affect the blocking occurrence by changing the tropospheric circulations.

In addition, these wintertime atmospheric circulations, such as AO and SSW, are closely associated with autumn snow cover variation (Cohen and Entekhabi 1999, 2001; Cohen and Fletcher 2007; Cohen et al. 2002, 2007, 2014; Smith et al. 2011). These previous studies suggested that the autumn snow cover anomaly over the Eurasia continent may enhance the vertical propagation of planetary waves through the expansion of the high pressure system over the Siberian region, which results in a weakened stratospheric polar vortex. The associated stratospheric circulation plays an important role in modulating the occurrence of the negative AO. Kryjov (2015) has also shown that autumn snow cover anomalies over northern Eurasia are closely associated with the October circulation anomaly over the Taymyr Peninsula, which can impact the wintertime atmospheric circulation. Similarly, Kim et al. (2014) have found that stratospheric variability in response to reduced Arctic sea ice is a vital element in modulating the wintertime AO mode. In particular, the AO in January and February modulated by the variation of stratospheric polar vortex can result in a vertical linkage structure ranging from the ground to the stratosphere (Kodera et al. 2000). The above studies suggest that the blocking phenomenon is related not only to the troposphere but also to the stratospheric circulations in the Northern Hemisphere, and that the autumn snow cover anomaly could act as a forcing on wintertime BF via changing the planetary wave activity in the boreal winter.

In this study, we focus on the role of boreal late autumn snow cover, especially over western and central China, in modulating the Northern Hemisphere wintertime BFs. This region includes the Tibetan Plateau (TP) and the East Asian westerly jet. According to the previous studies, the orographic forcing of the TP is known to play an important role in the formation of stationary planetary waves that propagate into the

stratosphere in the Northern Hemisphere (Plumb 1985). In addition, many studies have also emphasized the thermal effects of the TP on atmospheric circulation (Li and Yanai 1996; Duan and Wu 2005). In fact, thermal forcing over the TP, such as changes in snow cover, has been found to significantly affect the position and intensity of the East Asian westerly jet by modulating the tropospheric meridional temperature gradient (Kuang and Zhang 2005; Kuang et al. 2007; Zhang et al. 2004). This zonal wind distribution, induced by thermal forcing over the TP, may enhance the vertical propagation of planetary waves (Dickinson 1968; Matsuno 1970).

Based on these aforementioned studies, the autumn snow cover over western and central China, centered in the TP, may plausibly modulate the wintertime atmospheric circulations. However, most existing studies (Bamzai and Shukla 1999; Ao and Sun 2016) have merely examined the relationship between climate variations over Asia and snow cover over eastern Europe, rather than snow cover over western and central China. Therefore, it is necessary to analyze the snow cover over western and central China as a precursor of Northern Hemisphere wintertime BFs. The present study analyzes the characteristics of the Northern Hemisphere wintertime blocking phenomenon and examines the predictability of BFs using the relationship between the Northern Hemisphere blocking and the autumn snow cover anomaly in the western and central China regions.

The paper is organized as follows. In section 2, the data used in this study are briefly introduced and the blocking index is defined in detail. The relationship between the western and central China autumn snow cover and the Northern Hemisphere BF for winter is addressed in section 3. The mechanism of this lag correlation is explained in section 4. Finally, in section 5, the study is summarized.

2. Data and method

a. Data

The present study utilizes daily- and monthly-mean atmospheric variables provided by the National Centers for Environmental Prediction (NCEP)–National Center for Atmospheric Research (NCAR) reanalysis with a horizontal resolution of 2.5° × 2.5° (Kalnay et al. 1996). The monthly-mean snow cover data are derived from the National Oceanic and Atmospheric Administration (NOAA)/Cooperative Institute for Research in Environmental Sciences (CIRES) Twentieth Century Reanalysis (20CR, version 2; Compo et al. 2011), which has a horizontal resolution of approximately 2.0° in both latitudinal and longitudinal directions. The 20CR

provides a continuous record of the global snow cover data, which are widely used for climate analyses. By comparing this snow data with a large number of in situ observations, Peings et al. (2013) have proven that 20CR snow cover data are reliable for assessing the snow–atmosphere interaction over the entire twentieth century. He and Wang (2016) have used 20CR snow cover data to assess the role of Eurasian snow cover in linking the East Asian January temperature and preceding wintertime AO. The analysis period in this study is confined to 1958–2012 because NCEP–NCAR reanalysis data are more reliable since 1958 when the modern rawinsonde network was established (Kistler et al. 2001), and the 20CR data are available from January 1871 through December 2012 on the NOAA website at https://www.esrl.noaa.gov/psd/data/gridded/data.20thC_ReanV2.html. To confirm our results derived from 20CR snow data, we also used NOAA satellite snow cover product obtained from the Rutgers University Global Snow Laboratory (http://climate.rutgers.edu/snowcover/) during overlapping periods from 1967 to 2012.

Monthly indices of the AO (Thompson and Wallace 1998, 2000) and NAO (Barnston and Livezey 1987) are obtained from the NOAA Climate Prediction Center website (http://www.cpc.ncep.noaa.gov/) for the same period. The vertical Eliassen–Palm fluxes (EPF) defined by Plumb (1985) are calculated to analyze the effect of upward propagating planetary waves on the stratospheric polar vortex. To find the active region of the East Asian westerly jet, we calculated the number of jet core occurrences at each grid point of 300 hPa during November for 1958–2012, as defined by Ren et al. (2010) and Zhang and Chen (2017). A jet core is identified if 1) the horizontal wind speed is greater than $30\,\mathrm{m\,s}^{-1}$ and 2) the wind speed at the central point is larger than the surrounding eight grid points.

b. Definition of the Eady growth rate

We define the Eady growth rate, which is widely used to assess the baroclinic instability in the troposphere (Eady 1949; Lindzen and Farrell 1980; Simmonds and Lim 2009). The rate is closely related to vertical wind shear in the troposphere through the thermal wind relationship. The Eady growth rate is defined as follows:

$$\sigma = 0.31 \frac{f}{N} \left| \frac{\partial v}{\partial z} \right|, \qquad (1)$$

where f denotes the Coriolis parameter, N the buoyancy frequency, v the wind velocity, and z the vertical height.

The Eady growth rate is calculated from the layer between 1000 and 200 hPa because baroclinic instability occurs predominantly in the troposphere.

c. Definition of the blocking index

Over the past several decades, many studies have attempted to objectively identify the blocked atmospheric flows in various ways. An objective blocking index was first introduced by Lejenäs and Økland (1983). Based on this index, Tibaldi and Molteni (1990) newly defined a blocking index. Another form of this index, which is modified and supplemented by Barriopedro et al. (2006), is the most widely used currently (You and Ahn 2012; Park and Ahn 2014). In the present study, following Barriopedro et al. (2006) and You and Ahn (2012), blocking is defined in terms of meridional geopotential height gradients, using daily-mean 500-hPa geopotential height data for 55 years from 1958 to 2012.

The northern and southern 500-hPa geopotential height gradients (GHGN and GHGS, respectively) are simultaneously computed for each longitude and for each day as follows:

$$\mathrm{GHGN}(\lambda) = \frac{Z(\lambda, \phi_N) - Z(\lambda, \phi_0)}{\phi_N - \phi_0} \quad \text{and} \qquad (2)$$

$$\mathrm{GHGS}(\lambda) = \frac{Z(\lambda, \phi_0) - Z(\lambda, \phi_S)}{\phi_0 - \phi_S}, \qquad (3)$$

where $Z(\lambda, \phi)$ is the 500-hPa geopotential height at longitude λ and at a given latitude ϕ as follows:

$$\begin{aligned} \phi_N &= 77.5°\mathrm{N} + \Delta, \\ \phi_0 &= 60.0°\mathrm{N} + \Delta, \quad \text{and} \\ \phi_S &= 40.0°\mathrm{N} + \Delta, \end{aligned} \qquad (4)$$

where $\Delta = -5.0°, -2.5°, 0.0°, 2.5°,$ or $5.0°$.

The five results for GHGN(λ) and GHGS(λ) are computed by applying the five Δ. A given longitude is considered to be blocked at a given time when both GHGN and GHGS satisfy the condition expressed by (5) for at least one of the five different latitudes:

$$\mathrm{GHGN} < -10\,\mathrm{gpm}\,(°\mathrm{lat})^{-1} \text{ and } \mathrm{GHGS} > 0\,\mathrm{gpm}\,(°\mathrm{lat})^{-1}. \qquad (5)$$

In addition, a blocking event is defined to have occurred at that longitude if these conditions are satisfied for at least five consecutive days. BF is represented as the ratio of blocking days to the total number of days of winter (Barriopedro et al. 2006).

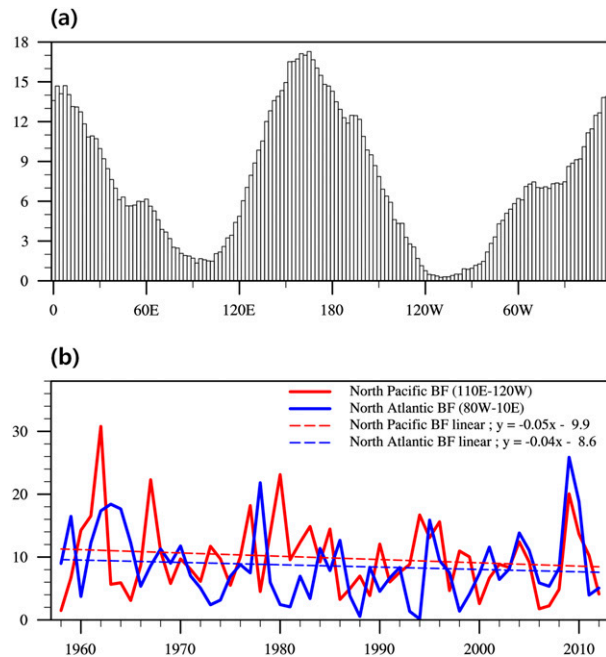Figure 1a shows climatological wintertime BF over the Northern Hemisphere as a function of the longitude.

FIG. 1. (a) Climatological wintertime blocking frequency (BF), and (b) time series of North Pacific (red) and North Atlantic (blue) BFs for 1958–2012. The dashed lines in (b) indicate the linear regression lines as described by the equations in the figure.
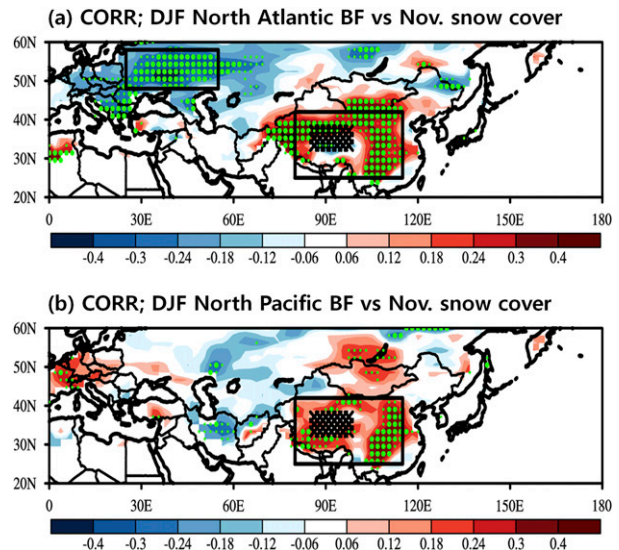

FIG. 2. Correlations between the November snow cover anomalies and (a) DJF North Atlantic BF and (b) DJF North Pacific BF for 1958–2012. The large (small) green dots in (a) and (b) indicate the areas where correlation coefficients are significant at the 95% (90%) confidence level. Areas at higher altitudes in the Tibetan Plateau where the snow cover variability is small are excluded from the analysis.

3. Basic statistical analyses

a. Linear relationships between the late autumn snow cover anomaly and wintertime blocking frequency

The winter blocking occurs frequently in the North Pacific (110°E–120°W) and North Atlantic (80°W–10°E), but less in the vicinity of 90°E and 110°W. This result is consistent with that of previous studies, indicating that blocking events mainly occur at the exit zones of the storm tracks in the Northern Hemisphere (Rex 1950b; Dole and Gordon 1983; Knox and Hay 1985; Barriopedro et al. 2010, You and Ahn 2012; Dunn-Sigouin and Son 2013). The two major blocking regions with high frequency (North Pacific and North Atlantic) are analyzed in the present study, although the frequency of European blocking (10°–60°E) is also high. The zonally averaged BFs for two longitude bands (North Pacific and North Atlantic) are defined as the North Pacific BF index (NP_BFI) and the North Atlantic BF index (NA_BFI), respectively. Figure 1b shows the time series of NP_BFI and NA_BFI. The time-averaged frequency of the occurrence of North Pacific blocking (9.9%) is higher than that of North Atlantic blocking (8.6%). Both NP_BFI and NA_BFI exhibit interannual to interdecadal fluctuations embedded in the long-term decreasing trend. In particular, the decreasing tendency of NP_BFI is slightly larger than that of NA_BFI. Although an investigation of this finding may be worthwhile, it is beyond the scope of this study.

In the present study, correlation analyses are conducted to analyze the effects of the late autumn snow cover anomaly on the wintertime blocking occurrence over the North Atlantic and North Pacific. Figure 2a (Fig. 2b) shows the correlation patterns between NA_BFI (NP_BFI) and the November snow cover anomaly. A dipole-type pattern between southeastern and northwestern Eurasia is revealed in Fig. 2a. The significant positive snow cover anomalies associated with both wintertime BFs (North Pacific and North Atlantic BFs) are located over East Asia with the maximum centered in western and central China (right black rectangles in Figs. 2a and 2b), whereas the negative snow cover anomalies related to NA_BFI are centered in eastern Europe (left black rectangle in Fig. 2a). Similarly, weak negative snow cover anomalies, associated with NP_BFI, are located to the north of the Black and Caspian Seas. That is, there is no strong covariability between the series of eastern Europe snow cover and NP_BFI, with the correlation coefficient being as negligible as −0.08, whereas the correlation coefficients between November snow cover anomalies over western and central China and both NA_BFI and NP_BFI exceed the 95% confidence threshold.
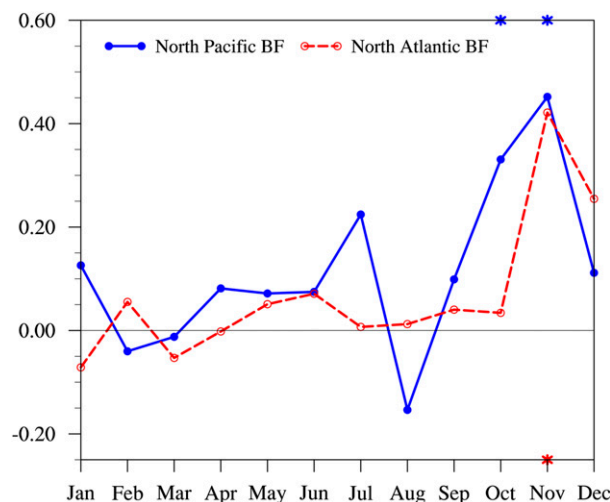
FIG. 3. Lag correlation coefficients between monthly snow cover indices (SCIs) over western and central China and wintertime (DJF) North Pacific BF (solid blue) and North Atlantic BF (dashed red). The values that are statistically significant at the 95% confidence level are indicated by an asterisk.
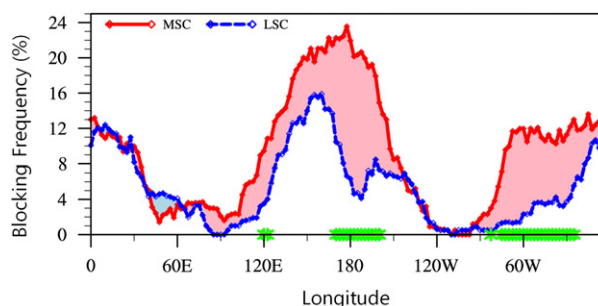

FIG. 4. Composite of DJF blocking frequencies (BFs) for November SCI based on the upper quintile (MSC in western and central China) and the lower quintile (LSC). Red (blue) shading denotes that the values in solid line are greater (less) than values in the dashed line. The green asterisks indicate the areas where correlation coefficients are significant at the 90% confidence level.

To characterize the interannual variability of the obtained pattern of snow cover anomalies, we have constructed a monthly snow cover index (SCI) by area-averaging the snow cover anomalies over western and central China, a region where the correlation coefficients between November snow cover anomalies and both NP_BFI and NA_BFI exceed the 95% confidence level. However, the areas at higher altitudes in the TP where the snow cover variability is small are excluded from the averaging, since the statistical relationships between November snow cover anomalies over this confined region and both BFs are weak. Figure 3 shows the lag correlation of the two Northern Hemisphere wintertime BF indices (NP_BFI and NA_BFI) with monthly SCIs. As can be seen from the figure, the wintertime BFs and SCI show high correlation coefficients when there are 1- or 2-month time lags. In particular, the linkages between wintertime NP_BFI and SCIs for the preceding October and November are evident with the correlation coefficients reaching 0.31 and 0.45, which are significant at the 95% and 99% confidence levels, respectively. In addition, the correlation coefficient between November SCI and NA_BFI is 0.42, which is significant at the 99% confidence level. On the contrary, SCIs for January through September show relatively low correlations with NP_BFI and NA_BFI. These statistical results suggest that November snow cover anomalies can potentially induce changes in Northern Hemisphere wintertime BFs with time lags. In the present study, November SCI is identified as a precursor to wintertime BFs by averaging the SCIs during the early snowy season in western and central China.

b. Composite analysis for the wintertime blocking

To examine the effect of late autumn snow cover variability over western and central China on the wintertime blocking occurrence in the Northern Hemisphere, composite analysis is conducted (Fig. 4). We base the composites on the quintile (20th percentile) method. This method distributes a set of values into five groups that contain an equal number of samples. The upper and lower quintiles in the normalized November SCI from 1958 to 2012 are defined as the cases of more snow cover (MSC) and less snow cover (LSC) in western and central China, respectively. The frequencies of the blocking occurrence over the North Pacific and North Atlantic are higher during the MSC years than during the LSC years. The differences are significant at the 90% confidence level, especially over the regions marked with green asterisks. These results are consistent with the correlation analyses in Figs. 2 and 3, indicating that November snow cover anomalies over western and central China may affect the blocking occurrence in the North Pacific and North Atlantic regions.

To determine the effects of November snow cover anomalies over western and central China on the duration of the blocking event over the two major blocking regions (North Pacific and North Atlantic), the composites of BFs as a function of duration are analyzed for the MSC and LSC years separately. The blue and red bars presented in Fig. 5 show the results of composite analysis for NP_BFI and NA_BFI, respectively. The results indicate that the frequencies of blocking occurrence are higher during MSC years than during LSC years. That is, the positive anomalous snow cover in the

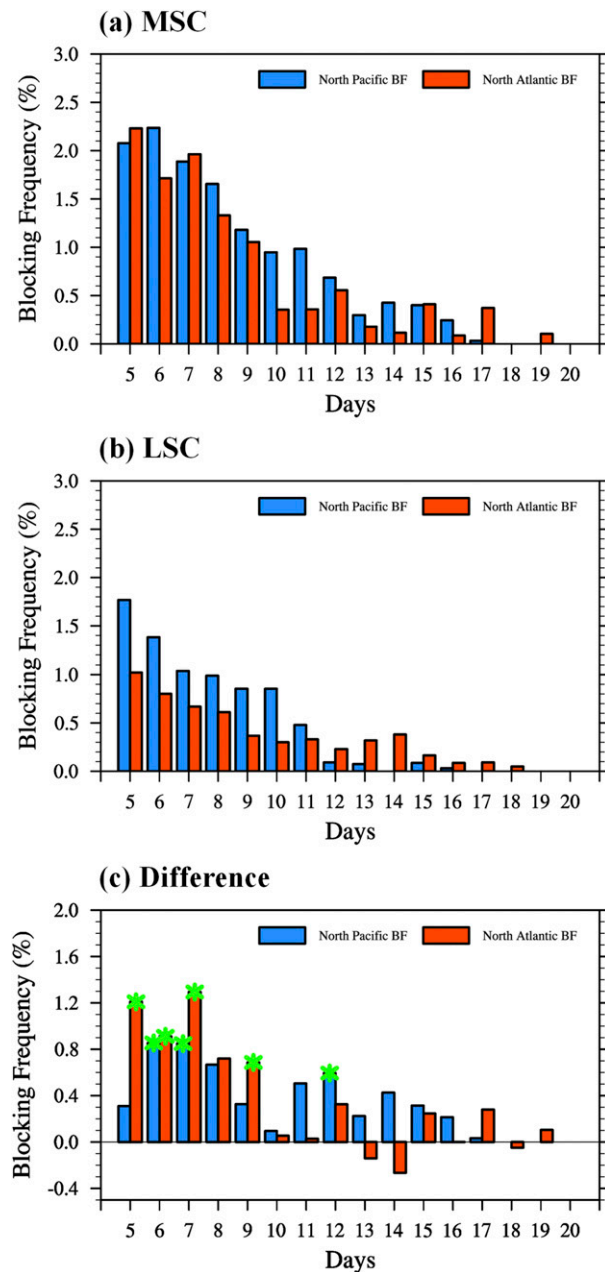## (a) MSC

(b) LSC

(c) Difference

FIG. 5. Frequency distribution of blocking duration longer than five days in the North Pacific (blue) and North Atlantic (red) regions for (a) the upper quintile (MSC), (b) the lower quintile (LSC), and (c) their difference (MSC minus LSC). The green asterisks indicate the differences that are significant at the 90% confidence level.

western and central China regions during late autumn may increase the BF over the North Pacific, regardless of duration. In particular, the largest increases in BF over the North Pacific are revealed in the shorter duration group (days 6–7), which is significant at the 90% confidence level. Meanwhile, after the late autumn of the

positive anomalous snowfall in western and central China, short-lived (less than 10-day duration) blocking events are mainly increased over the North Atlantic with the largest increases in BF of 5–7-day and 9-day durations. That is, the frequencies of North Atlantic blocking having duration longer than 10 days are not significantly correlated with November SCI. This contrast between responses of BFs may be due to differences in the blocking mechanisms at work in the North Pacific and North Atlantic, although comprehensive understanding will require future study. In line with this, several previous studies proposed differences in blocking mechanisms between North Pacific and North Atlantic blocks (e.g., Kim and Ha 2015).

The correlation analysis is performed to quantitatively investigate the relationships among November SCI, wintertime BFs, and the dominant wintertime climate variability in the Northern Hemisphere such as DJF AO and DJF NAO (Table 1). The correlation coefficient between NA_BFI and November SCI is 0.42, which is significant at the 99% confidence level. In addition, the correlation coefficient between NA_BFI and DJF AO is −0.58 and between NA_BFI and DJF NAO is −0.79, which are both significant at the 99% confidence level. Meanwhile, NP_BFI shows relatively low correlations with wintertime AO and NAO, which is in line with Shabbar et al. (2001). These results imply that a number of autumn precursors of the wintertime AO, such as the snow cover extent index (e.g., Cohen and Fletcher 2007; Cohen et al. 2007), snow advance index (Cohen and Jones 2011), and Taymyr circulation index (Kryjov 2015; Kryjov and Min 2016), may be reasonable predictors for North Atlantic blocking. Furthermore, the correlation coefficient between NP_BFI and November SCI is 0.45, which is significant at the 99% confidence level. The above results are confirmed by the analysis of satellite-based snow cover data. The correlation coefficient between November SCI derived from Rutgers snow cover data and NP_BFI (NA_BFI) is 0.37 (0.30), which is significant at the 95% (95%) confidence level. These correlations not only support the hypothesis that November snow cover anomalies can potentially induce changes in Northern Hemisphere wintertime BFs, but also support the reliability of the 20CR snow cover data.

4. Possible mechanisms

The correlation and composite analyses have shown that the November snow cover anomalies over western and central China may act as a precursor of Northern Hemisphere wintertime BFs. When the November SCI is positive (negative), blocking occurrence in the North

TABLE 1. Correlation coefficients among November SCI, DJF AO, DJF NAO, NP_BFI, and NA_BFI for 1958–2012. The values in parentheses indicate the correlation coefficients obtained from Rutgers snow cover data during the overlapping period from 1967 to 2012. One asterisk indicates significance at the 95% confidence level and two asterisks indicate significance at the 99% confidence level.

	NP_BFI	NA_BFI	DJF AO	DJF NAO
November SCI	0.45** (0.37*)	0.42** (0.30*)	−0.57** (−0.48**)	−0.51** (−0.32*)
NP_BFI		0.09	−0.26	−0.13
NA_BFI			−0.58**	−0.79**
DJF AO				0.78**

Pacific and North Atlantic regions increases (decreases) during boreal wintertime. However, the mechanisms for the lag relationship between wintertime BFs and November SCI have not been studied yet. We propose the stratosphere–troposphere interactions excited by the thermal forcing of snow cover as a possible mechanism for the relationship. That is, thermal forcing, induced by anomalous snow cover over the western and central China regions, could affect the tropospheric circulation during late autumn, resulting in favorable conditions for wintertime blocking through the stratosphere–troposphere interaction. Such a mechanism has already been proposed in several previous papers based on observations and model experiments. Matsuno (1971) has suggested that planetary waves, induced in the troposphere, can trigger SSW through dynamical processes. In addition, Baldwin and Dunkerton (1999, 2001) have presented observational evidence indicating that SSW may affect tropospheric circulations through stratosphere–troposphere interactions. Based on this, Saito et al. (2001) have found that autumn (September– November) Eurasian snow cover may enhance the vertical propagation of Rossby waves, which may affect the extratropical Northern Hemisphere climate variability. Studies conducted by Garfinkel et al. (2010) and Smith et al. (2011) have further suggested that wavenumber-1 and wavenumber-2 components of the height field, produced by the orographic and thermal forcing of the Northern Hemisphere, can affect EPF in the lower stratosphere when they are in phase with climatological height fields. This EPF in turn weakens the polar vortex. These studies suggest that the constructive interference between the climatological long planetary waves (e.g., Fig. 2 of Garfinkel et al. 2010) and the forced troughs excited by the thermal forcing of snow cover over western and central China (this thermal forcing is discussed in more detail below) may provide a favorable condition to affect the wintertime BFs through the stratosphere–troposphere interaction.

The correlation analysis is conducted to examine the effects of November snow cover anomalies on atmospheric circulations in the upper troposphere and lower stratosphere (Fig. 6). The positive snow cover anomalies

in western and central China during late autumn reduce the solar radiation absorbed at the surface, leading to local cooling that can decrease the 300–1000-hPa thickness (Fig. 6a). The associated thickness anomalies
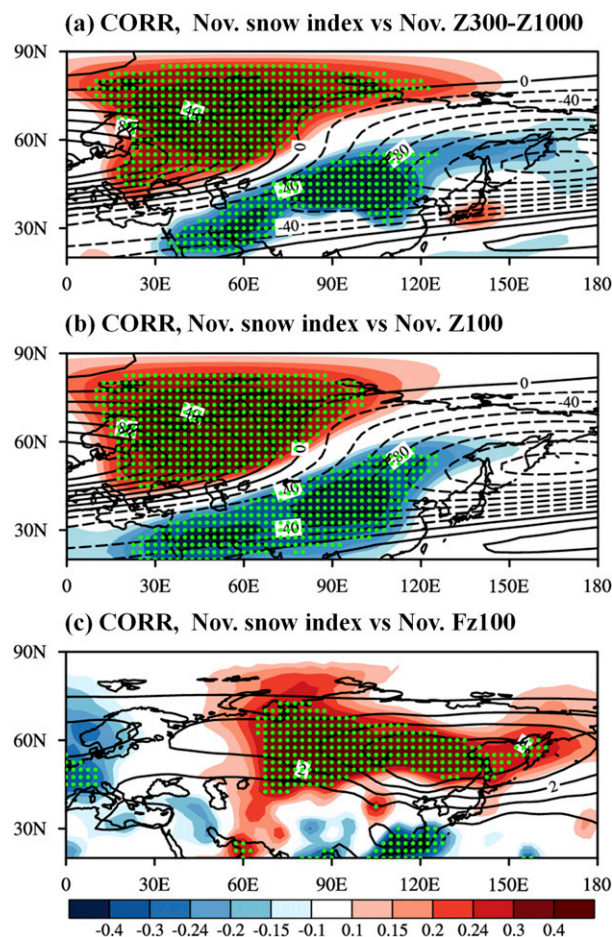

FIG. 6. Correlations (shading) between November snow cover index (SCI) and (a) the November 300–1000-hPa layer thickness, (b) November Z100, and (c) November upward 100-hPa EPF for 1958–2012. The contour lines in (a) and (b) denote the climatological wavenumber-1 height field at 300 hPa (m) and those shown in (c) indicate the climatology of vertical Plumb wave flux (10^3 m^2 s^{-2}) at 100 hPa. Positive and negative values are shown by solid and dashed lines, respectively. The green dots exhibit the areas where correlation coefficients are significant at the 95% confidence level.
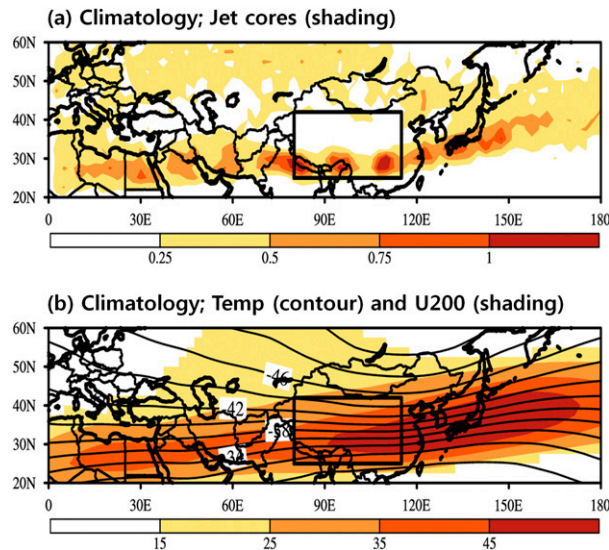
FIG. 7. (a) The number of jet core occurrences at each grid point of 300 hPa during November for 1958–2012, and (b) the climatological-mean temperature (°C) in the upper tropospheric layers (200–500 hPa; contour) and zonal wind (m s^{-1}) distribution at 200 hPa (shading).
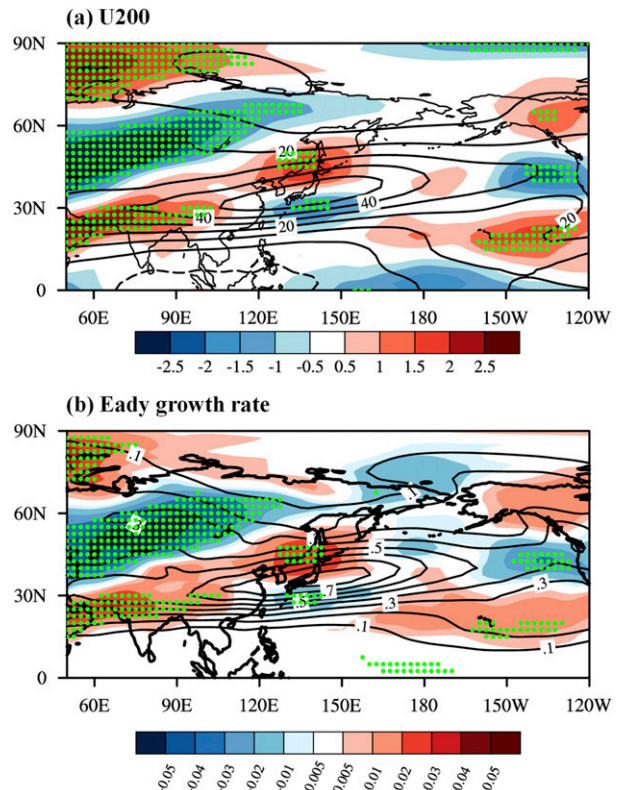

FIG. 8. Regression of the (a) November zonal wind anomaly at 200 hPa and (b) the November Eady growth rate anomaly on the November SCI. The green dots indicate the areas where the correlation coefficients are significant at the 95% confidence level. The contour lines in (a) and (b) denote the November climatological zonal wind at 200 hPa and the Eady growth rate between 1000 and 200 hPa, respectively.

in turn significantly decrease the geopotential height in the lower stratosphere (Fig. 6b), which gives rise to the constructive interference between the forced (shading of Fig. 6b) and climatological (contour line of Fig. 6b) waves. This interference enhances the upward propagating EPF to the stratosphere, especially over northeastern Eurasia (Fig. 6c) where the major planetary wave activity center is located (contour line of Fig. 6c). These results are in line with previous studies (Smith et al. 2011; Kryjov 2015; Kryjov and Min 2016; Kim et al. 2014) and support our hypothesis that the stratosphere–troposphere interaction links the wintertime BFs and the boreal late autumn snow cover over western and central China.

In addition to the change in atmospheric thickness anomaly, we examine the relationship between November snow cover anomalies over western and central China and East Asian westerly jets. Figure 7 shows that the East Asian polar front jet is mainly located over the poleward side of the TP, while the East Asian plateau jet is situated at the southern side of the TP. The two jets merge over southern Japan (Fig. 7a), resulting in strong upper-level zonal wind centered at the southern part of Japan (Fig. 7b). Although the major center of the East Asian subtropical jet is located over the northern Pacific, we focused on the polar front jet located over the north of the TP and the plateau jet located over the southern flank of the TP.

Figure 8a shows the regression map of November 200-hPa zonal wind anomalies on the November SCI.

The snow cover anomalies in the western and central China regions may significantly affect the intensity of the East Asian westerly jet (Fig. 8a). That is, positive snow cover anomalies over western and central China can decrease (increase) the latitudinal temperature gradients over the poleward (southern) side of the TP, weakening the East Asian polar front jet in the vicinity of 50°N (strengthening the plateau jet over the southern side of the TP), according to the thermal wind relationships. These correspond to the increased (decreased) baroclinicity in the vicinity of 25°N (50°N) (Fig. 8b). These results are in line with Liao and Zhang (2013), who found a concurrent variation between the East Asian plateau jet and the polar front jet during persistent snowstorm periods. This concurrent variation between the East Asian plateau jet and the polar front jet in turn generates the cyclonic circulation anomaly (Fig. 6b) through the changes in upper layer winds (Fig. 8a). This dynamical mechanism is explained by previous studies (Wang et al. 2014; Huang et al. 2015; Choi et al. 2016). The associated
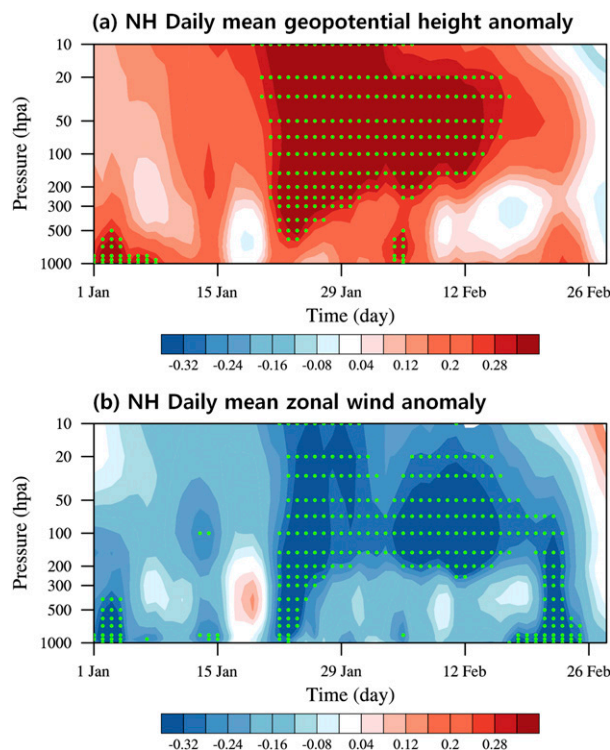
FIG. 9. Time–height cross section of 35°–90°N averaged (a) geopotential height and (b) zonal wind anomalies regressed onto the November SCI. The green dots indicate the areas where the correlation coefficients are significant at the 95% confidence level.
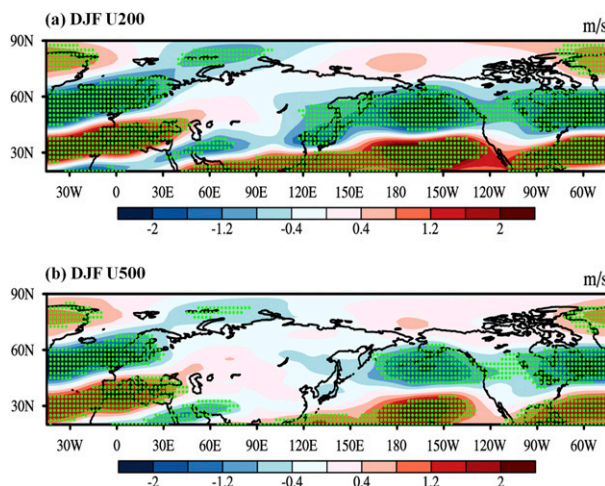

FIG. 10. Regression of the zonal wind anomalies at (a) 200 and (b) 500 hPa on the November SCI. The green dots indicate the areas where the correlation coefficients are significant at the 95% confidence level.

cyclonic circulations in the lower stratosphere increase the EPF (Fig. 6c), which propagates into the stratosphere through the constructive interference between the forced and climatological waves (Garfinkel et al. 2010; Smith et al. 2011). These upward-propagating planetary waves, associated with the dipole anomaly in the geopotential height field, can decelerate the stratospheric jet by collapsing of the polar vortex in the stratosphere (Charney and Drazin 1961). These phenomena are discussed in more detail below.

Thus far, it has been shown that the positive (negative) snow cover anomalies over western and central China increase (decrease) the upward-propagating tropospheric waves. To identify the coupling between the stratosphere and the troposphere, regression analysis is conducted. Figure 9 shows the time–height cross section of the area-averaged geopotential height (Fig. 9a) and zonal wind (Fig. 9b) anomalies in the Northern Hemisphere (35°–90°N, all longitudes) regressed onto the November SCI. The region is where the blocks are most frequent climatologically and these two area-averaged anomalies are closely related to the polar vortex variability. In particular, positive (negative) geopotential

height and negative (positive) zonal wind anomalies correspond to a weakened (strengthened) polar vortex. During early January, positive (negative) geopotential height anomalies dominate the whole troposphere with a maximum value in the lower troposphere. These positive (negative) geopotential height anomalies extend to the upper stratosphere through stratosphere–troposphere coupling, which in turn propagates back into the troposphere in mid-January. In relation to this result, the decreased (increased) zonal wind speed in the upper layer of the BF region induces favorable synoptic conditions that can easily develop (dissipate) wintertime blocking (Fig. 9b). These results indicate that November snow cover anomalies in the western and central China regions may affect the formation of wintertime blocking through the stratosphere–troposphere interactions. Several studies have also suggested that the autumn Eurasia snow cover is closely related to vertically propagating planetary waves, which weaken the stratospheric polar vortex (Cohen and Entekhabi 1999, 2001; Cohen and Fletcher 2007; Cohen et al. 2002, 2007, 2014).

Figure 10 shows the regression map of upper-layer zonal wind anomalies on the November SCI. We found that positive (negative) snow cover anomalies in the western and central China regions weaken (strengthen) the stratospheric polar vortex, which in turn affects the tropospheric atmospheric variability. The weakened (strengthened) stratospheric circulation anomaly, propagating from the stratosphere to the troposphere, significantly weakens (strengthens) upper-layer zonal winds in the North Pacific and North Atlantic regions where the wintertime blocking phenomenon is most
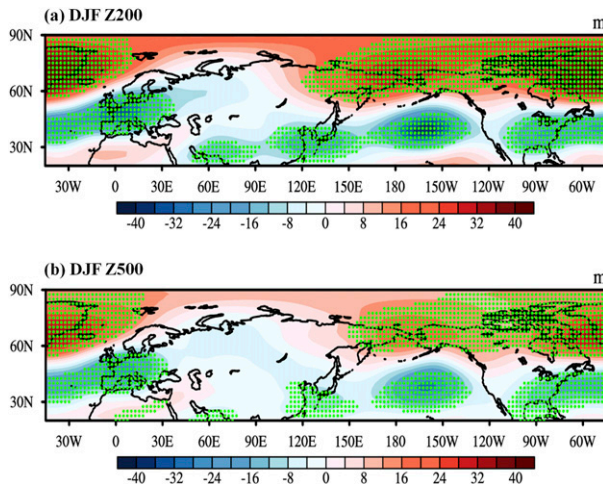
FIG. 11. Regression of the geopotential height anomalies at (a) 200 and (b) 500 hPa on the November SCI. The green dots indicate the areas where the correlation coefficients are significant at the 95% confidence level.

active (Fig. 10). Concurrently, the atmospheric pressure field and weather system moving eastward becomes stagnant, which increases BF.

The regression map of the geopotential height anomalies on the November SCI yields a barotropic structure, which bears some resemblance with the AO (Fig. 11). Particularly, positive geopotential height anomalies prevail over the polar cap region (north of 60°N), whereas negative anomalies occur south of 60°N in the Northern Hemisphere, with the largest negative anomalies being located over the North Pacific and North Atlantic. That is, November SCI reduces the meridional geopotential height gradient and thus induces favorable conditions for blocking, especially over the North Pacific and North Atlantic where the climatological blocks are most frequent.

5. Summary

The present study has examined the effects of November snow cover anomalies over western and central China on the formation of wintertime Northern Hemisphere blocking. Our findings reveal that wintertime atmospheric circulations induced by late autumn snow cover anomalies form favorable conditions for increased BF, especially in the North Pacific and North Atlantic. We also found evidence that the stratosphere–troposphere interactions, which are modulated by snow cover, especially over western and central China (centered in the TP), seem to be the key mechanism of the lag response of wintertime North Pacific and North Atlantic BFs to the late autumn snow cover.

A set of statistical results demonstrate that the positive (negative) November SCI tends to be followed by increased (decreased) Northern Hemisphere BFs. That is, NP_BFI, NA_BFI, and November SCI significantly covariate over the entire period, with correlation coefficients of 0.45 between November SCI and NP_BFI and of 0.42 between November SCI and NA_BFI, which are significant at the 99% confidence level. To further verify that the Northern Hemisphere BFs are associated with snow cover variation over western and central China, composite analysis based on the quintiles was conducted. The frequencies of blocking occurrence are higher during MSC years than during LSC years, especially over the North Pacific and North Atlantic. In addition, the positive anomalous snow cover in the western and central China regions during late autumn increases BF over the North Pacific, regardless of duration with the largest increases in BF occurring in the shorter durations (days 6–7). Meanwhile, BF with duration less than 10 days is increased over the North Atlantic with a significant (90%) increase in BF for shorter durations (days 5–7 and 9).

The key component for the mechanism of the lag response of wintertime BFs to the late autumn snow cover is the stratosphere–troposphere interactions, which are modulated by snow cover, especially over western and central China, centered in the TP. The positive (negative) anomalous snow cover in the western and central China regions during late autumn can induce a dipole anomaly in the geopotential height field over the lower stratosphere, with a positive (negative) pole over northwestern Eurasia and a negative (positive) pole over western and central China, due to both the decrease (increase) of the 300–1000-hPa thickness over western and central China and the concurrent variation between the East Asian plateau jet and the polar front jet. The corresponding atmospheric circulations below the stratosphere, induced by snow cover anomalies, increase (decrease) the upward propagating EPF to the stratosphere through constructive (destructive) interference between the forced and climatological waves. This EPF weakens (strengthens) the polar vortex in the stratosphere, which affects the tropospheric circulation through the stratosphere–troposphere interactions. That is, the weakened (strengthened) stratospheric polar vortex may induce upper-level easterly (westerly) wind anomalies in the North Pacific and North Atlantic regions where the wintertime blocking phenomenon is most active. In turn, the atmospheric pressure field and weather system moving eastward become stagnant (active) to form favorable (unfavorable) conditions for blocking.

These results reveal the linkages among the autumn snow cover and wintertime stratospheric and tropospheric circulations, and demonstrate that BF is probably predictable to some extent. In conclusion, the SCI may be applied for skillful seasonal climate predictions, despite the difficulty in detailed forecasting of individual blocking events. Additional studies using climate models may provide more explicit support for the statistical relationship between snow cover and wintertime BF.

REFERENCES

Ambrizzi, T., and B. J. Hoskins, 1997: Stationary Rossby-wave propagation in a baroclinic atmosphere. *Quart. J. Roy. Meteor. Soc.*, **123**, 919–928, doi:10.1002/qj.49712354007.

Ao, J., and J. Sun, 2016: Connection between November snow cover over Eastern Europe and winter precipitation over East Asia. *Int. J. Climatol.*, **36**, 2396–2404, doi:10.1002/joc.4484.

Baldwin, M., and T. J. Dunkerton, 1999: Propagation of the Arctic Oscillation from the stratosphere to the troposphere. *J. Geophys. Res.*, **104**, 30 937–30 946, doi:10.1029/1999JD900445.

——, and ——, 2001: Stratospheric harbingers of anomalous weather regimes. *Science*, **294**, 581–584, doi:10.1126/science.1063315.

Bamzai, A. S., and J. Shukla, 1999: Relation between Eurasian snow cover, snow depth, and the Indian summer monsoon: An observational study. *J. Climate*, **12**, 3117–3132, doi:10.1175/1520-0442(1999)012<3117:RBESCS>2.0.CO;2.

Barnston, A. G., and R. E. Livezey, 1987: Classification, seasonality and persistence of low frequency atmospheric circulation patterns. *Mon. Wea. Rev.*, **115**, 1083–1126, doi:10.1175/1520-0493(1987)115<1083:CSAPOL>2.0.CO;2.

Barriopedro, D., R. García-Herrera, A. R. Lupo, and E. Hernández, 2006: A climatology of Northern Hemisphere blocking. *J. Climate*, **19**, 1042–1063, doi:10.1175/JCLI3678.1.

——, ——, and R. M. Trigo, 2010: Application of blocking diagnosis methods to general circulation models. Part I: A novel detection scheme. *Climate Dyn.*, **35**, 1373–1391, doi:10.1007/s00382-010-0767-5.

Black, E., M. Blackburn, G. Harrison, B. Hoskins, and J. Methven, 2004: Factors contributing to the summer 2003 European heatwave. *Weather*, **59**, 217–223, doi:10.1256/wea.74.04.

Buehler, T., C. C. Raible, and T. F. Stocker, 2011: The relationship of winter season North Atlantic blocking frequencies to extreme cold or dry spells in the ERA-40. *Tellus*, **63A**, 212–222, doi:10.1111/j.1600-0870.2010.00492.x.

Charney, J. G., and P. G. Drazin, 1961: Propagation of planetary-scale disturbances from the lower into the upper atmosphere. *J. Geophys. Res.*, **66**, 83–109, doi:10.1029/JZ066i001p00083.

——, J. Shukla, and K. C. Mo, 1981: Comparison of a barotropic blocking theory with observation. *J. Atmos. Sci.*, **38**, 762–779, doi:10.1175/1520-0469(1981)038<0762:COABBT>2.0.CO;2.

Choi, Y. W., J. B. Ahn, and V. N. Kryjov, 2016: November seesaw in northern extratropical sea level pressure and its linkage to the preceding wintertime Arctic Oscillation. *Int. J. Climatol.*, **36**, 1375–1386, doi:10.1002/joc.4431.

Cohen, J., and D. Entekhabi, 1999: Eurasian snow cover variability and Northern Hemisphere climate predictability. *Geophys. Res. Lett.*, **26**, 345–348, doi:10.1029/1998GL900321.

——, and ——, 2001: The influence of snow cover on Northern Hemisphere climate variability. *Atmos.–Ocean*, **39**, 35–53, doi:10.1080/07055900.2001.9649665.

——, and C. Fletcher, 2007: Improved skill of Northern Hemisphere winter surface temperature predictions based on land–atmosphere fall anomalies. *J. Climate*, **20**, 4118–4132, doi:10.1175/JCLI4241.1.

——, and J. Jones, 2011: A new index for more accurate winter predictions. *Geophys. Res. Lett.*, **38**, L21701, doi:10.1029/2011GL049626.

——, D. Salstein, and K. Saito, 2002: A dynamical framework to understand and predict the major Northern Hemisphere mode. *Geophys. Res. Lett.*, **29**, 1412, doi:10.1029/2001GL014117.

——, M. Barlow, P. J. Kushner, and K. Saito, 2007: Stratosphere–troposphere coupling and links with Eurasian land surface variability. *J. Climate*, **20**, 5335–5343, doi:10.1175/2007JCLI1725.1.

——, J. C. Furtado, J. Jones, M. Barlow, D. Whittleston, and D. Entekhabi, 2014: Linking Siberian snow cover to precursors of stratospheric variability. *J. Climate*, **27**, 5422–5432, doi:10.1175/JCLI-D-13-00779.1.

Colucci, S. J., and T. L. Alberta, 1996: Planetary-scale climatology of explosive cyclogenesis and blocking. *Mon. Wea. Rev.*, **124**, 2509–2520, doi:10.1175/1520-0493(1996)124<2509:PSCOEC>2.0.CO;2.

Compo, G. P., and Coauthors, 2011: The Twentieth Century Reanalysis Project. *Quart. J. Roy. Meteor. Soc.*, **137**, 1–28, doi:10.1002/qj.776.

Dickinson, R. E., 1968: Planetary Rossby waves propagating vertically through weak westerly wind wave guides. *J. Atmos. Sci.*, **25**, 984–1002, doi:10.1175/1520-0469(1968)025<0984:PRWPVT>2.0.CO;2.

Dole, R. M., and N. D. Gordon, 1983: Persistent anomalies of the extratropical Northern Hemisphere wintertime circulation: Geographical distribution and regional persistence characteristics. *Mon. Wea. Rev.*, **111**, 1567–1586, doi:10.1175/1520-0493(1983)111<1567:PAOTEN>2.0.CO;2.

Duan, A. M., and G. X. Wu, 2005: Role of the Tibetan Plateau thermal forcing in the summer climate patterns over subtropical Asia. *Climate Dyn.*, **24**, 793–807, doi:10.1007/s00382-004-0488-8.

Dunn-Sigouin, E., and S.-W. Son, 2013: Northern Hemisphere blocking frequency and duration in the CMIP5 models. *J. Geophys. Res. Atmos.*, **118**, 1179–1188, doi:10.1002/jgrd.50143.

Eady, E. T., 1949: Long waves and cyclone waves. *Tellus*, **1**, 33–52, doi:10.3402/tellusa.v1i3.8507.

Garfinkel, C. I., D. L. Hartmann, and F. Sassi, 2010: Tropospheric precursors of anomalous Northern Hemisphere stratospheric polar vortices. *J. Climate*, **23**, 3282–3299, doi:10.1175/2010JCLI3010.1.

He, S., and H. Wang, 2016: Linkage between the East Asian January temperature extremes and the preceding Arctic Oscillation. *Int. J. Climatol.*, **36**, 1026–1032, doi:10.1002/joc.4399.

He, Y., J. Huang, and M. Ji, 2014: Impact of land–sea thermal contrast on interdecadal variation in circulation and blocking. *Climate Dyn.*, **43**, 3267–3279, doi:10.1007/s00382-014-2103-y.

Hoskins, B. J., and P. D. Sardeshmukh, 1987: A diagnostic study of the dynamics of the Northern Hemisphere winter of 1985–86. *Quart. J. Roy. Meteor. Soc.*, **113**, 759–778, doi:10.1002/qj.49711347705.

——, and T. Ambrizzi, 1993: Rossby wave propagation on a realistic longitudinally varying flow. *J. Atmos. Sci.*, **50**, 1661–1671, doi:10.1175/1520-0469(1993)050<1661:RWPOAR>2.0.CO;2.

Huang, D.-Q., J. Zhu, Y.-C. Zhang, J. Wang, and X.-Y. Kuang, 2015: The impact of the East Asian subtropical jet and polar front jet on the frequency of spring persistent rainfall over southern China in 1997–2011. *J. Climate*, **28**, 6054–6066, doi:10.1175/JCLI-D-14-00641.1.

Kalnay, E., and Coauthors, 1996: The NCEP–NCAR 40-Year Reanalysis Project. *Bull. Amer. Meteor. Soc.*, **77**, 437–471, doi:10.1175/1520-0477(1996)077<0437:TNYRP>2.0.CO;2.

Kim, B.-M., S.-W. Son, S.-K. Min, J.-H. Jeong, S.-J. Kim, X. Zhang, T. Shim, and J.-H. Yoon, 2014: Weakening of the stratospheric polar vortex by Arctic sea-ice loss. *Nat. Commun.*, **5**, 4646, doi:10.1038/ncomms5646.

Kim, H.-J., and J.-B. Ahn, 2015: Improvement in prediction of the Arctic Oscillation with a realistic ocean initial condition in a CGCM. *J. Climate*, **28**, 8951–8967, doi:10.1175/JCLI-D-14-00457.1.

Kim, S.-H., and K.-J. Ha, 2015: Two leading modes of Northern Hemisphere blocking variability in the boreal wintertime and their relationship with teleconnection patterns. *Climate Dyn.*, **44**, 2479–2491, doi:10.1007/s00382-014-2304-4.

Kistler, R., and Coauthors, 2001: The NCEP–NCAR 50-Year Reanalysis: Monthly means CD-ROM and documentation. *Bull. Amer. Meteor. Soc.*, **82**, 247–267, doi:10.1175/1520-0477(2001)082<0247:TNNYRM>2.3.CO;2.

Knox, J. L., and J. E. Hay, 1985: Blocking signatures in the Northern Hemisphere: Frequency distribution and interpretation. *Int. J. Climatol.*, **5**, 1–16, doi:10.1002/joc.3370050102.

Kodera, K., Y. Kuroda, and S. Pawson, 2000: Stratospheric sudden warmings and slowly propagating zonal-mean zonal wind anomalies. *J. Geophys. Res.*, **105**, 12 351–12 359, doi:10.1029/2000JD900095.

Kryjov, V. N., 2015: October circulation precursors of the wintertime Arctic Oscillation. *Int. J. Climatol.*, **35**, 161–171, doi:10.1002/joc.3968.

——, and Y.-M. Min, 2016: Predictability of the wintertime Arctic Oscillation based on autumn circulation. *Int. J. Climatol.*, **36**, 4181–4186, doi:10.1002/joc.4616.

Kuang, X. Y., and Y. C. Zhang, 2005: Seasonal variation of the East Asian subtropical westerly jet and its association with the heating field over East Asia. *Adv. Atmos. Sci.*, **22**, 831–840, doi:10.1007/BF02918683.

——, ——, and J. Liu, 2007: Seasonal variation of the East Asian subtropical westerly jet and the thermal mechanism. *Acta Meteor. Sin.*, **21**, 192–203, http://www.cmsjournal.net:8080/Jweb_jmr/EN/Y2007/V21/I2/192.

Kung, E. C., C. C. Dacamara, W. E. Baker, J. Susskind, and C. K. Park, 1990: Simulations of winter blocking episodes using observed sea surface temperatures. *Quart. J. Roy. Meteor. Soc.*, **116**, 1053–1070, doi:10.1002/qj.49711649503.

Lejenäs, H., and H. Økland, 1983: Characteristics of Northern Hemisphere blocking as determined from a long time series of observational data. *Tellus*, **35**, 350–362, doi:10.3402/tellusa.v35i5.11446.

Li, C., and M. Yanai, 1996: The onset and interannual variability of the Asian summer monsoon in relation to land–sea thermal contrast. *J. Climate*, **9**, 358–375, doi:10.1175/1520-0442(1996)009<0358:TOAIVO>2.0.CO;2.

Liao, Z., and Y. Zhang, 2013: Concurrent variation between the East Asian subtropical jet and polar front jet during persistent snowstorm period in 2008 winter over southern China. *J. Geophys. Res. Atmos.*, **118**, 6360–6373, doi:10.1002/jgrd.50558.

Lindzen, R. S., and B. Farrell, 1980: A simple approximate result for the maximum growth rate of baroclinic instabilities. *J. Atmos. Sci.*, **37**, 1648–1654, doi:10.1175/1520-0469(1980)037<1648:ASARFT>2.0.CO;2.

Luo, D., 2005: Why is the North Atlantic block more frequent and long-lived during the negative NAO phase? *Geophys. Res. Lett.*, **32**, L20804, doi:10.1029/2005GL022927.

Matsuno, T., 1970: Vertical propagation of stationary planetary waves in the winter Northern Hemisphere. *J. Atmos. Sci.*, **27**, 871–883, doi:10.1175/1520-0469(1970)027<0871:VPOSPW>2.0.CO;2.

——, 1971: A dynamical model of the stratospheric sudden warming. *J. Atmos. Sci.*, **28**, 1479–1494, doi:10.1175/1520-0469(1971)028<1479:ADMOTS>2.0.CO;2.

Mullen, S. L., 1987: Transient eddy forcing of blocking flows. *J. Atmos. Sci.*, **44**, 3–22, doi:10.1175/1520-0469(1987)044<0003:TEFOBF>2.0.CO;2.

Nakamura, H., and J. M. Wallace, 1993: Synoptic behavior of baroclinic eddies during the blocking onset. *Mon. Wea. Rev.*, **121**, 1892–1903, doi:10.1175/1520-0493(1993)121<1892:SBOBED>2.0.CO;2.

Park, Y.-J., and J.-B. Ahn, 2014: Characteristics of atmospheric circulation over East Asia associated with summer blocking. *J. Geophys. Res. Atmos.*, **119**, 726–738, doi:10.1002/2013JD020688.

Peings, Y., E. Brun, V. Mauvais, and H. Douville, 2013: How stationary is the relationship between Siberian snow and Arctic Oscillation over the 20th century? *Geophys. Res. Lett.*, **40**, 183–188, doi:10.1029/2012GL054083.

Plumb, R. A., 1985: On the three-dimensional propagation of stationary waves. *J. Atmos. Sci.*, **42**, 217–229, doi:10.1175/1520-0469(1985)042<0217:OTTDPO>2.0.CO;2.

Ren, X. J., X. Q. Yang, and C. J. Chu, 2010: Seasonal variations of the synoptic-scale transient eddy activity and polar front jet over East Asia. *J. Climate*, **23**, 3222–3233, doi:10.1175/2009JCLI3225.1.

Renwick, J. A., 1998: ENSO-related variability in the frequency of South Pacific blocking. *Mon. Wea. Rev.*, **126**, 3117–3123, doi:10.1175/1520-0493(1998)126<3117:ERVITF>2.0.CO;2.

——, and J. M. Wallace, 1996: Relationships between North Pacific wintertime blocking, El Niño, and the PNA pattern. *Mon. Wea. Rev.*, **124**, 2071–2076, doi:10.1175/1520-0493(1996)124<2071:RBNPWB>2.0.CO;2.

Rex, D. F., 1950a: Blocking action in the middle troposphere and its effect upon regional climate. Part I: An aerological study of blocking action. *Tellus*, **2**, 196–211, doi:10.1111/j.2153-3490.1950.tb00331.x.

——, 1950b: Blocking action in the middle troposphere and its effect upon regional climate. Part II: The climatology of blocking action. *Tellus*, **2**, 275–301, doi:10.1111/j.2153-3490.1950.tb00339.x.

Saito, K., J. Cohen, and D. Entekhabi, 2001: Evolution in atmospheric response to early-season Eurasian snow cover

anomalies. *Mon. Wea. Rev.*, **129**, 2746–2760, doi:10.1175/1520-0493(2001)129<2746:EOARTE>2.0.CO;2.

Shabbar, A., J. Huang, and K. Higuchi, 2001: The relationship between the wintertime North Atlantic Oscillation and blocking episodes in the North Atlantic. *Int. J. Climatol.*, **21**, 355–369, doi:10.1002/joc.612.

Shutts, G. J., 1983: The propagation of eddies in diffluent jet streams: Eddy vorticity forcing of blocking flow fields. *Quart. J. Roy. Meteor. Soc.*, **109**, 737–761, doi:10.1002/qj.49710946204.

Simmonds, I., and E. P. Lim, 2009: Biases in the calculation of Southern Hemisphere mean baroclinic Eady growth rate. *Geophys. Res. Lett.*, **36**, L01707, doi:10.1029/2008GL036320.

Smith, K. L., P. J. Kushner, and J. Cohen, 2011: The role of linear interference in northern annular mode variability associated with Eurasian snow cover extent. *J. Climate*, **24**, 6185–6202, doi:10.1175/JCLI-D-11-00055.1.

Song, Y., and W. A. Robinson, 2004: Dynamical mechanisms for stratospheric influences on the troposphere. *J. Atmos. Sci.*, **61**, 1711–1725, doi:10.1175/1520-0469(2004)061<1711:DMFSIO>2.0.CO;2.

Sun, J., and J.-B. Ahn, 2015: Dynamical seasonal predictability of the Arctic Oscillation using a CGCM. *Int. J. Climatol.*, **35**, 1342–1353, doi:10.1002/joc.4060.

Thompson, D. W. J., and J. M. Wallace, 1998: The Arctic Oscillation signature in the wintertime geopotential height and temperature fields. *Geophys. Res. Lett.*, **25**, 1297–1300, doi:10.1029/98GL00950.

——, and ——, 2000: Annular modes in the extratropical circulation. Part I: Month-to-month variability. *J. Climate*, **13**, 1000–1016, doi:10.1175/1520-0442(2000)013<1000:AMITEC>2.0.CO;2.

Tibaldi, S., and F. Molteni, 1990: On the operational predictability of blocking. *Tellus*, **42**, 343–365, doi:10.3402/tellusa.v42i3.11882.

Trigo, R. M., R. García-Herrera, J. Díaz, I. F. Trigo, and M. A. Valente, 2005: How exceptional was the early August 2003 heatwave in France? *Geophys. Res. Lett.*, **32**, L10701, doi:10.1029/2005GL022410.

Tyrrell, G. C., D. J. Karoly, and J. L. McBride, 1996: Links between tropical convection and variations of the extratropical circulation during TOGA COARE. *J. Atmos. Sci.*, **53**, 2735–2748, doi:10.1175/1520-0469(1996)053<2735:LBTCAV>2.0.CO;2.

Wang, W., W. Zhou, and D. Chen, 2014: Summer high temperature extremes in southeast China: Bonding with the El Niño–Southern Oscillation and East Asian summer monsoon coupled system. *J. Climate*, **27**, 4122–4138, doi:10.1175/JCLI-D-13-00545.1.

Woollings, T., A. Charlton-Perez, S. Ineson, A. G. Marshall, and G. Masato, 2010: Associations between stratospheric variability and tropospheric blocking. *J. Geophys. Res.*, **115**, D06108, doi:10.1029/2009JD012742.

You, J. E., and J. B. Ahn, 2012: The anomalous structures of atmospheric and oceanic variables associated with the frequency of North Pacific winter blocking. *J. Geophys. Res.*, **117**, D11108, doi:10.1029/2012JD017431.

Zhang, Y., and J. Chen, 2017: Characterizing the winter concurrent variation patterns of the subtropical and polar-front jets over East Asia. *J. Meteor. Res.*, **31**, 160–170, doi:10.1007/s13351-016-6094-y.

——, T. Li, and B. Wang, 2004: Decadal change of the spring snow depth over the Tibetan Plateau: The associated circulation and influence on the East Asian summer monsoon. *J. Climate*, **17**, 2780–2793, doi:10.1175/1520-0442(2004)017<2780:DCOTSS>2.0.CO;2.